The Nephroprotective Effect of MS-275 on Lipopolysaccharide (LPS)-Induced Acute Kidney Injury by Inhibiting Reactive Oxygen Species (ROS)-Oxidative Stress and Endoplasmic Reticulum Stress

Authors' Contribution:
Study Design A
Data Collection B
Statistical Analysis C
Data Interpretation D
Manuscript Preparation E
Literature Search F
Funds Collection G

BCD 1 Haiyue Zhang*
CF 1 Wenbin Zhang*
CD 1 Fangzhou Jiao
CD 1 Xun Li
DF 2 Hong Zhang
EF 1 Luwen Wang
A 1 Zuojiong Gong

1 Department of Infectious Diseases, Renmin Hospital of Wuhan University, Wuhan, Hubei, P.R. China
2 Department of Pharmaceutical, Renmin Hospital of Wuhan University, Wuhan, Hubei, P.R. China

* Haiyue Zhang, and Wenbin Zhang contributed equally this work
Corresponding Author: Zuojiong Gong, e-mail: zjgong@163.com
Source of support: This study was supported by a grant from the National Natural Science Foundation of China (No. 81371789)

Background: Histone deacetylase (HDAC) inhibitors can attenuate acute kidney injury (AKI)-mediated damage and reduce fibrosis in kidney disease models. The aim of the present study was to investigate the effects of the HDAC inhibitor MS-275 on lipopolysaccharide (LPS)-induced AKI and the associated mechanisms.

Material/Methods: A LPS-induced model in 6–8 weeks-old mice was established by intraperitoneal injection of LPS (10 mg/kg), with pre-treatment of MS-275 (2 mg/kg/day) administered intraperitoneally for five days. In addition, HK-2 cells were exposed to LPS (1 μg/mL) at 0.1 nM, 1 nM, 10 nM, and 100 nM. For our *in vitro* MS-275 study, detection programs included histology, biochemical, immunohistochemistry, mRNA and protein expression as well as apoptosis.

Results: MS-275 ameliorated renal damage, enhanced the survival rate of the LPS-induced sepsis model, decreased the expressions of TNF-α, IL-1β, IL-6, COX-2, and NF-κBp65 nucleus translocation, suppressed the HDAC activity which was enhanced in septic AKI mice, and enhanced the acetylation of histone H3 and H4. Reactive oxygen species (ROS) production was enhanced in the kidney of LPS mice compared to control mice, while MS-275 suppressed the production of ROS in kidney tissue. In the *in vitro* studies, MS-275 reduced the LPS-induced apoptosis of HK-2 cells, inhibited ROS and MDA production, increased the production GSH and SOD activity, decreased the expressions of CHOP, GRP78, caspase3, and capase12, which was related to endoplasmic reticulum stress in LPS stimulated HK-2 cells.

Conclusions: MS-275 pre-treatment improved renal function and ameliorated histological alterations, inflammation, and ROS production in LPS-induced AKI mice and may act through inhibiting ROS-oxidative stress and endoplasmic reticulum stress.

MeSH Keywords: Acute Kidney Injury • Endoplasmic Reticulum Stress • Oxidative Stress • Sepsis

Full-text PDF: https://www.medscimonit.com/abstract/index/idArt/906362

📄 3198   🗎 1   📊 7   📖 41

Background

Sepsis is defined as a type of systemic inflammatory response syndrome caused by the invasion of pathogenic bacteria or conditional pathogenic bacteria in the blood. The development of sepsis involves inflammatory cytokines and reactive oxygen species (ROS) production, which is caused by the migration of lymphocytes, leukocytes, and platelets to the infected areas and induces endothelial damage, microvascular permeability, platelet aggregation, local blood flow reduction, and then ischemia/reperfusion injury, leading to multiple organ failure [1–5]. Sepsis is often accompanied by acute kidney injury (AKI), which increases the risk of mortality during the uncontrolled systemic inflammatory response [6]. Exacerbated ROS production leads to AKI through ROS-induced abnormal signal pathway, inflammatory infiltration, cellular dysfunction, and renal cell death [7,8]. ROS generation may induce three types of programmed cell death: pyroptosis, apoptosis, and autophagy. Abnormal apoptosis of renal tubular epithelial cells may affect the occurrence and progression of AKI [9,10]. ROS induces apoptosis by activating Bax expression/caspase-3 activity/poly-(ADP-ribose)-polymerase (PARP) fragments [7]. At present, effective prevention and treatment for septic AKI is limited. Studies have indicated that inhibition of apoptosis/autophagy or induction of autophagy is a potential new target for therapeutic exploration of sepsis [11–13]. Endoplasmic reticulum (ER) stress occurs when unfolded proteins accumulate and the homeostasis of the ER is lost. Numerous studies have reported the relationship between ER stress and kidney diseases; ER stress response has become a major focus of kidney disease research [14,15].

Histone deacetylase (HDAC) inhibitors have a pivotal effect on nerve protection, anti-oxidation, viscera protection, and anti-inflammatory response [16–19]. HDACs play multiple roles during both kidney development and the pathogenesis of kidney disease [20–23]. Liu and Zhuang reported that HDAC inhibitors protect against chronic kidney disease through multiple mechanisms involving anti-inflammation, immunosuppressive, prevention of apoptosis, prevention of proliferation, reduction of vasculitis and anti-fibrosis [24]. In the present study, we used MS-275 (selectively inhibiting class I HDACs activity), to investigate the effects of HDAC inhibitors on the AKI in a LPS-induced septic model and explored the underling mechanisms.

Material and Methods

Reagents included: MS-275 (Selleck, USA); LPS (Sigma-Aldrich Co., USA); BUN, and creatinine commercially obtained kits (Jiancheng Bioengineering Institute, Nanjing, China); TNF-α, IL-1β, and IL-6 ELISA kits (eBioscience, California, USA); reverse transcription and PCR assay kit (Takara Bio Inc., Japan); SYBR Green real-time PCR kit (Takara Bio Inc., Japan); PCR primers (Biofavor Biotech, China); ROS fluorescent probe-dihydroethidium (Vigorous Biotechnology Beijing Co., Ltd., China); primary antibody of NF-κBp65, H3, H4, growth arrest, and DNA damage inducible 153 (CHOP), GAPDH (Cell Signaling Technology, Inc, Danvers, MA, USA); β-actin (Boster Biological Technology Co. Ltd., China); glucose-regulated protein 78 (GRP78) and caspase12 (Abcam, UK); caspase3 (Proteintech Group, Inc, China); secondary antibody (rabbit and mouse) (LICOR Co., USA); BCA protein concentration determination kit (Biosharp, China); reactive oxygen species (ROS) assay kit, malondialdehyde (MDA) assay kit, super oxide dismutase (SOD) assay kit and glutathione (GSH) assay kit (Naijing Jiancheng Bioengineering Institute, China); Annexin V-FITC apoptosis detection kit (KeyGen BioTech Co. Ltd., China); DMEM/F12 (HyClone, USA); and FBS (Gibico, Australia).

Animal models

Specific pathogen free (SPF) C57BL/6 mal mice, 6–8 weeks old, weighing 20 to 25 g, were purchased from the Experimental Animal Center of Hubei Province. All animals were fed with a standard laboratory diet and acclimatized for five days before the experiment. The mice were given humanistic concern according to the animal laboratory guidelines.

Mice were divided into three groups at random: the MS-275 group with pre-treatment with MS-275 at 2 mg/kg/day by intraperitoneal injection for five days before LPS 10 mg/kg, intraperitoneal injection (n=32); the model LPS group with 10 mg/kg by intraperitoneal injection (n=32); and the control group with no injection (n=32). Half of the mice in each group were used to observe the survival rate in the 72 hours following LPS intraperitoneal injection; the rest of the mice were sacrificed, and serum and renal tissues were harvested at 24 hours and used for further study.

Cell cultures

Human renal proximal tubular cells (HK-2 cells), donated by Dr. Qi You in Renmin Hospital of Wuhan University, were cultured in 10% FBS-containing DMEM/F12 medium at 37°C in humidified atmosphere of 5% CO_2. HK-2 cells were pre-treated with MS-275 in concentrations of 0.1 nM, 1 nM, 10 nM, and 100 nM at two hours before treatment with LPS (1 μg/mL). Then 24 hours later, supernatant and cells were harvested for further analysis.

Histopathology and kidney function

Renal tissue was incised for 5 μm paraffin sections that were stained with hematoxylin and eosin (H&E) stain. The pathological changes were evaluated by BX51 light microscope (OLUMPUS, Japan).

Table 1. List of primer sequences used for quantitative polymerase chain reaction.

Gene	Primer sequence	
	Forward	Reverse
COx-2	GGTCTGGTGCCTGGTCTGATGATG	GTCCTTTCAAGGAGAATGGTGC
KIM-1	GGGTCTCCTTCACAGCACATT	AAGCACTGGGTACAGATCCAAA
NGAL	GGAAGAACCAAGGGGCTGTC	CGCTCACCGTCTGTTCAGTT
GAPDH	AGGAGCGAGACCCCACTAACA	AGGGGGGCTAAGCAGTTGGT

The serum BUN, creatinine, TNF-α, IL-1β, and IL-6 levels in mice were determined using ELISA kits according to the kit instructions, and assayed were performed using a microplate reader.

ROS expression in kidney tissue and HK-2 cells

The ROS expression in kidney tissue was evaluated by ROS fluorescent probe-dihydroethidium staining, according to the product instructions, then detected by fluorescence microscopy (Olympus BX51 DP73), with blue or green light excitation. ROS positive cells in the nuclear area were dyed red, and with ultraviolet excitation, the unoxidized dihydrogen in the cytoplasm emitted blue fluorescence.

The ROS production in HK-2 cells was detected using the dichloro-dihydro-fluorescein diacetate (DCFH-DA) method according to the ROS assay kit instructions and then the analysis was performed using a quantitative method via flow cytometry.

The detection of MDA, SOD, and GSH in HK-2 cells

MDA was detected by TBA method according to the MDA assay kit instructions. The expression of MDA was calculated using the following formula: MDA (nmol/mL)=[(OD$_{tested\ value}$−OD$_{control\ value}$)/(OD$_{standard\ value}$−OD$_{blank\ value}$)] × sample concentration × sample dilution ratio.

SOD was detected by WST-1 method according to the SOD assay kit instructions. The SOD inhibition ratio (%)=[(OD$_{control\ value}$−OD$_{control-blank\ value}$)/(OD$_{tested\ value}$−OD$_{tested-blank\ value}$)]/(OD$_{control\ value}$−OD$_{control-blank\ value}$). Then the SOD activity was calculated using the formula: SOD activity (U/mL)=SOD inhibition ratio/50% × dilution ratio × sample dilution ratio.

GSH was detected by micro-method according to the GSH assay kit instructions. The GSH expression was calculated using the following formula: GSH (µmol/L)=[(OD$_{tested\ value}$−OD$_{blank\ value}$)/(OD$_{standard\ value}$−OD$_{blank\ value}$)] × sample concentration × sample dilution ratio.

The distribution of NF-κB p65

The distribution of NF-κBp65 in the kidney was determined by immunohistochemistry. The method was described in a previous study [23]. The positive staining of NF-κBp65 was recognized as brown-yellow granules in cytoplasm or nuclei.

HDACs activity detection

The activity of HDACs in blood samples of mice were measured using an HDAC activity colorimetric assay kit (BioVision, Inc., Milpitas, CA, USA) according to the manufacturer's protocol. We then detect HDACs activity using a microplate reader.

Flow cytometry

The apoptosis of HK-2 cells was detected by flow cytometry (FCM) with Annexin V-FITC apoptosis detection kit, the expression of ROS in HK-2 cells was detected by FCM with ROS assay kit according to the kit instructions.

Quantitative real-time polymerase chain reaction

KIM-1, NGAL, and COX-2 in renal tissues were detected by quantitative real-time polymerase chain reaction (qPCR).

Total RNA was extracted from renal tissue, and reverse transcribed using Prime Script RT reagent kit with gDNA eraser. The q-PCR was performed with cDNA using the SYBR Green kit, gene-specific primers and a 7500 Sequence Detector System (Applied Biosystems, Foster City, CA, USA). The primers (Table 1) were developed with Primer Express software (Applied Biosystems). The relative quantification of RNA was calculated by $2^{-\Delta\Delta ct}$.

Western blotting

Protein extracts from renal tissue samples and HK-2 cells were performed to detect protein concentration using BCA protein concentration determination kit, then subjected to sodium dodecyl sulfate-polyacrylamide gel electrophoresis (SDS-PAGE), transferred to a polyvinylidene difluoride (PVDF) membrane
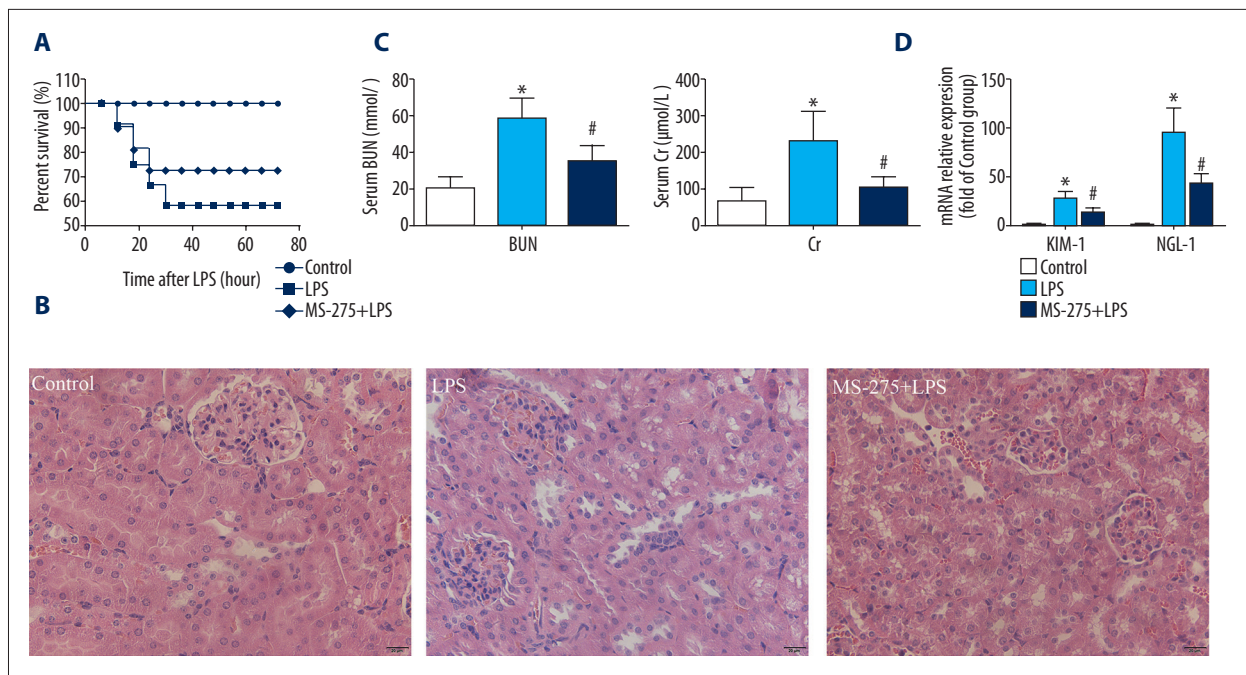
Figure 1. The survival rate and changes of histopathology and kidney function in 48 mice (16 mice in each group). (**A**) In the 72 hours after the intervention, the survival rate in the control group was 100%, in the LPS-induced AKI group it was 37.5% (6/16), in the MS-275 pre-treatment group it was 62.5% (10/16). MS-275 pre-treatment enhanced the survival rate of the LPS-induced AKI mice. (**B**) Swollen tubular epithelial cells and indistinct brush border were present in the LPS-induced AKI mice; MS-275 reduced swelling and vacuolar degeneration in the LPS-induced sepsis mice (magnification: 400×, calibration bar 20 μm). (**C**) BUN and creatinine were increased in LPS-induced AKI mice, but were suppressed by MS-275; * $p<0.05$ versus the control group; # $p<0.05$ versus the LPS group. (**D**) The expression of KIM-1 and NGAL in renal tissue was detected by qPCR. KIM-1 and NGAL were increased in the LPS group and MS-275 reduced the expression of KIM-1 and NGAL; * $p<0.05$ versus the control group; # $p<0.05$ versus the LPS group.

(Millipore, Merck KGaA, Darmstadt, Germany) then sealed with 5% skim milk powder at room temperature for one hour, and washed with PBS three times (five minutes per time). The membrane was sequential incubated with antibody of H3, H4, CHOP, caspase3, caspase12, and GRP78 at 4°C overnight, then washed with PBST three times (five minutes per time), and incubated with secondary antibody in the dark for one hour, washed with PBST three times (five minutes per time), and then detected by Odyssey infrared imaging system (LI-COR Co.). The gray-scale values reflected the expression of protein.

Statistical analysis

All measurement data were expressed as mean ± standard deviation (SD). Differences between groups were calculated by using one-way ANOVA with repeated measurements, followed by an Independent-Samples *t*-test. Results were considered statistically significant at $p<0.05$.

Results

The survival rate, histopathology, and kidney function

The 72-hour survival rate of LPS-induced mice was decreased to 37.5%; MS-275 enhanced the survival rate to 62.5% (Figure 1A). The histological changes in renal tissue were evaluated using H&E staining. Swollen tubular epithelial cells and indistinct brush border were present in the sepsis-induced AKI mice; MS-275 reduced swelling and vacuolar degeneration in LPS-induced sepsis mice (Figure 1B). MS-275 reduced the levels of BUN and creatinine in LPS-induced AKI mice (Figure 1C). KIM-1 and NGAL were considered markers of renal tubular injury. Compared to normal mice, mRNA expressions of KIM-1 and NGAL in the kidney of LPS-induced AKI mice were enhanced (Figure 1D). Implying that MS-275 ameliorated the renal injury in LPS-induced sepsis mice.

Inflammatory mediators

The expression of serum TNF-α, IL-1β, IL-6, and transcription of COX-2 in the renal tissue of sepsis-induced AKI mice were higher than normal mice. MS-275 significantly reduced TNF-α, IL-1β,
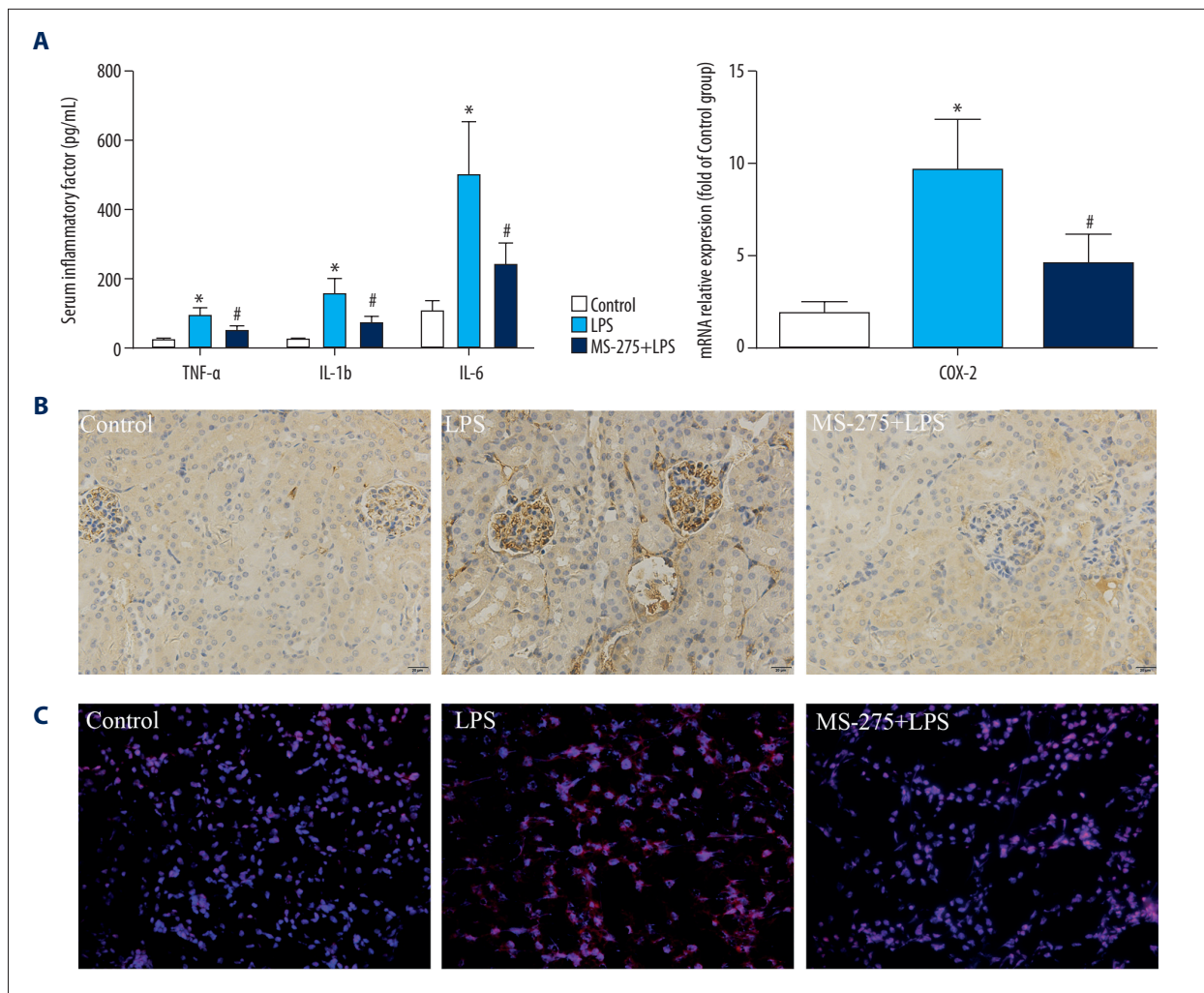
Figure 2. Inflammatory mediator expression in serum of 24 mice (six mice in the control group, eight mice in the LPS group, and 10 mice in MS-275+LPS group) and ROS expression in kidney tissues of three mice in each group. (**A**) The serum TNF-α, IL-1β, and IL-6 were detected by H&E; transcription of COX-2 in renal tissue was detected by qPCR. The inflammatory mediators were increased in LPS-induced AKI mice, but were suppressed by MS-275; * $p < 0.05$ versus the control group; # $p < 0.05$ versus the LPS group. (**B**) The expression of NF-κBp65 in renal tissue was detected by immunohistochemistry. In normal mice, NF-κBp65 was mainly detected in the cytoplasm of renal tissue; the density of NF-κBp65 was higher in both the nucleus and cytoplasm of sepsis-induced AKI mice; MS-275 reduced the density of NF-κBp65 in the nucleus of sepsis-induced AKI mice (400×). (**C**) The ROS expression presented as red fluorescence in the nuclei of cells, the blue fluorescence reflected the absence of ROS. The control group mainly manifested blue fluorescence; while, the red fluorescence was obviously stronger than blue fluorescence in the kidney of LPS mice, which implied substantial ROS generation; MS-275 attenuated the red fluorescence, indicating suppression of ROS generation (400×).

IL-6, and COX-2 levels in sepsis-induced AKI mice (Figure 2A). The distribution of NF-κBp65 in renal tissue was detected by immunohistochemistry. In normal mice, NF-κBp65 was mainly detected in the cytoplasm of renal tissue. The density of NF-κBp65 was higher in both the nucleus and cytoplasm in LPS-induced AKI mice. MS-275 reduced the density of NF-κBp65 in the nucleus of sepsis-induced AKI mice (Figure 2B). As a consequence, MS-275 reduced the inflammatory response in LPS-induced AKI mice.

The generation of ROS in mice

Dihydroethidium is free to enter the cell through the living cell membrane, and is oxidized by ROS in the cell to become ethylene oxide. Ethylene oxide can be incorporated into chromosomal DNA, producing red fluorescence, while, with ultraviolet excitation, the unoxidized dihydrogen in the cytoplasm can emit blue fluorescence. In the fluorescent images, the red fluorescence was more enhanced than the blue fluorescence in the kidneys of LPS mice compared to control mice, while
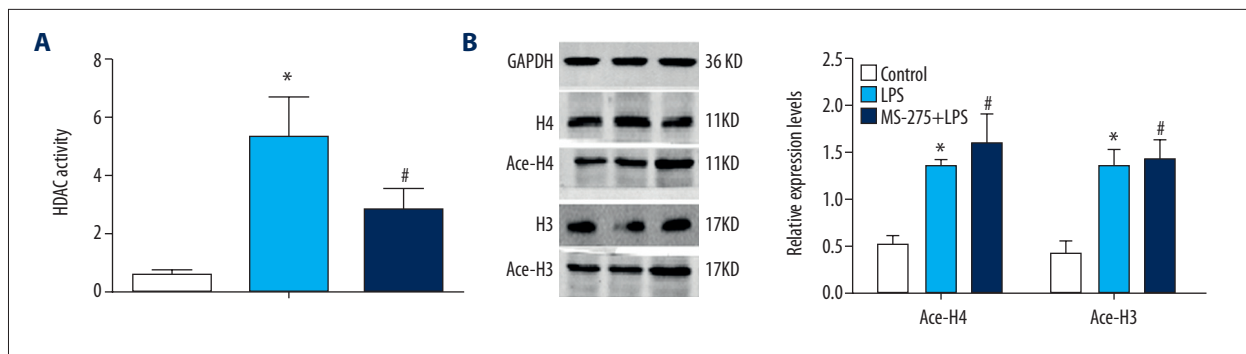
Figure 3. HDAC activity in serum and acetylation levels of histone H3 and H4 in kidney tissue of 24 mice (six mice in the control group, eight mice in the LPS group, and 10 mice in the MS-275+LPS group). (**A**) The HDAC activity in blood samples was enhanced in the LPS group, but was inhibited by MS-275. (**B**) The acetylation levels of H3 and H4 in renal tissue was enhanced by LPS and further enhanced by MS-275; * $p<0.05$ versus the control group; # $p<0.05$ versus the LPS group.

MS-275 weaken the red fluorescence in LPS mice (Figure 2C). This implied that MS-275 suppressed the generation of ROS in the kidneys of LPS-induced AKI mice.

HDAC activity and acetylation levels of histone H3 and H4

HDAC activity in sepsis-induced AKI mice was higher than in normal mice. MS-275 inhibited the HDAC activity of sepsis-induced AKI mice but was still higher than that of normal mice (Figure 3A). The expression of acetylated H3 and H4 were increased in LPS-induced AKI mice, and were enhanced further by MS-275 (Figure 3B).

Apoptosis of LPS-stimulated HK-2 cells

Apoptosis was detected by Annexin V-FITC apoptosis detection kit. The ratio of apoptosis was higher in LPS-stimulated HK-2 cells (Figure 4D) compared to the negative control (Figure 4A and 4B) and the normal control (Figure 4C). In the pre-treatment with the MS-275 group, with the increased concentration of MS-275 (0.1 nM, 1 nM, 10 nM, and 100 nM), early apoptosis began to decline at the concentration of 10 nM (Figure 4G); the late apoptosis began to decline at the concentration of 0.1 nM (Figure 4E), but increased at the concentration of 100 nM (Figure 4H). The apoptosis of LPS-stimulated HK-2 cells was suppressed by the increased concentration of MS-275 (within a certain range); when the concentration of MS-275 was 100 nM, the late apoptosis started to increase. We selected the 10 nM MS-275 for further study in the preliminary experiment.

The generation of ROS in HK-2 cells

The expression of ROS in HK-2 cells was represented by the mean fluorescence intensity (FITC-A) in the region of P1 (Figure 5A). The mean FITC-A in the LPS cells (13673095; Figure 5D) was higher compared to the negative control cells (1830.8; Figure 5B) and the normal cells (3917932; Figure 5C).

MS-275 suppressed ROS in LPS-stimulated HK-2 cells (7580892; Figure 5E).

Oxidative stress in LPS-stimulated HK-2 cells

MDA, one maker of oxidative stress, was enhanced in LPS-stimulated HK-2 cells, but suppressed by MS-275 (Figure 6A). Antioxidants, GSH expression, and SOD activity were decreased in LPS-stimulated HK-2 cells, but enhanced by MS-275 (Figure 6B, 6C).

Endoplasmic reticulum stress in LPS-stimulated HK-2 cells

CHOP and GRP78, which were considered important mediators and markers of ER stress, were enhanced in LPS-stimulated HK-2 cells, but were suppressed by MS-275 (Figure 7A). The expression of caspase3 (17KD) and caspase12 (36KD), which are the activated forms of caspase3 and caspase12 and involved in ER-induced apoptosis pathway, were enhanced in LPS-stimulated HK-2 cells, but were suppressed by MS-275. We did not find significant differences in caspase3 (32KD) and caspase12 (55KD) expression (inactivated forms of caspase3 and caspase12) between groups (Figure 7B).

Discussion

AKI is a leading cause of morbidity and mortality in patients with severe sepsis. Hence, there is an urgent need to investigate novel pharmacological interventions to treat or prevent AKI [24]. The generation of ROS and pro-inflammatory cytokines play key roles in sepsis AKI [25,26]. There is considerable evidence that oxidative damage to renal tissue and tubular cells is linked to AKI. Studies in sepsis patients with kidney injury or renal insufficiency have shown increased circulating biomarkers of lipid oxidation and protein that connected with markers of pro-inflammatory, pro-oxidative mediators, and
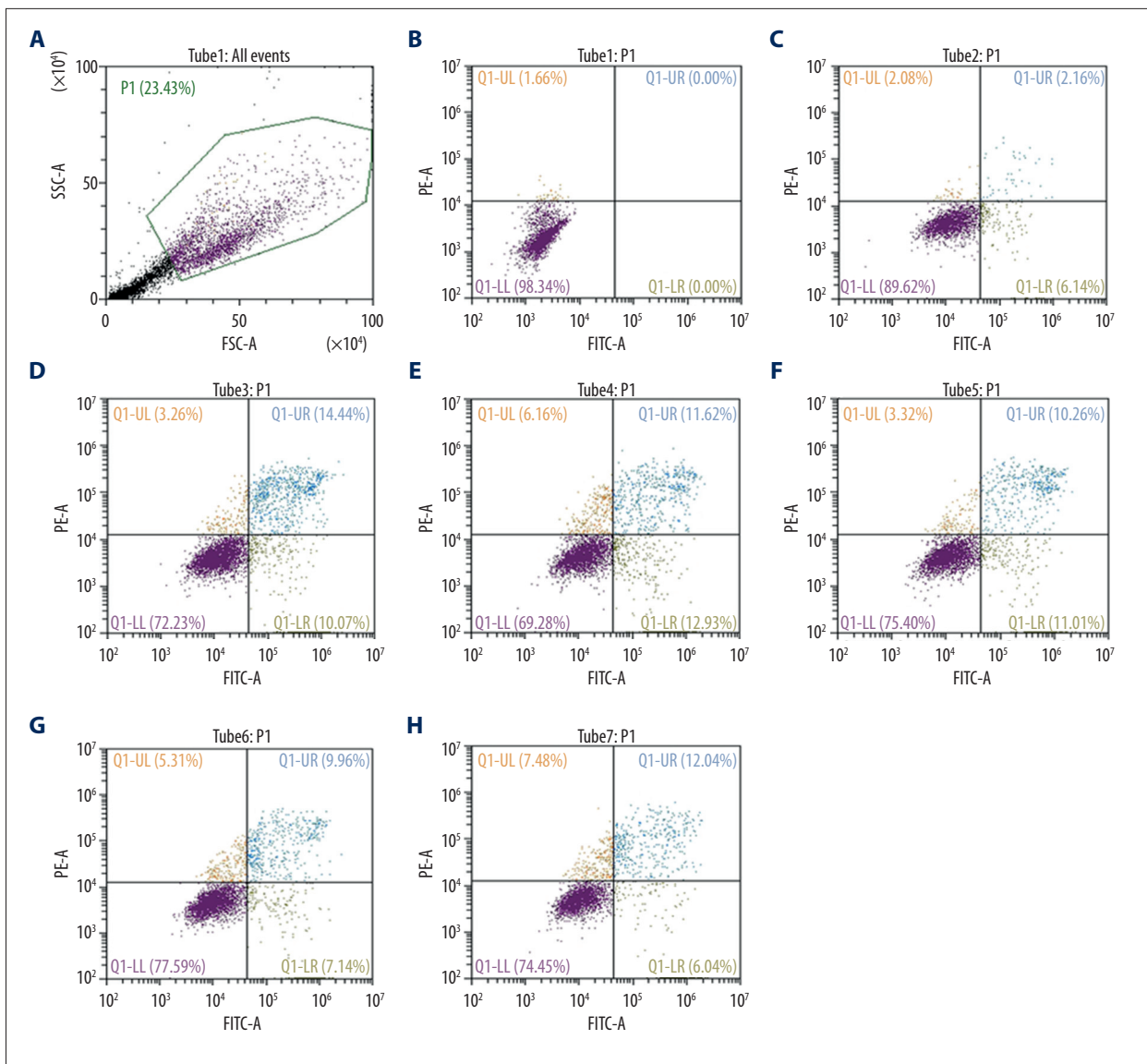
Figure 4. Apoptosis of LPS-stimulated HK-2 cells. (**A, B**) Negative control. (**B**) Normal control. (**C**) Apoptosis of LPS-stimulated HK-2 cells. The ratio of apoptosis was higher in HK-2 cells stimulated with LPS. (**D**) Pre-treatment with MS-275 at the concentration of 0.1 nM. (**E**) Pre-treatment with MS-275 at the concentration of 1 nM, (**F**) Pre-treatment with MS-275 at the concentration of 10 nM. (**G**) Pre-treatment with MS-275 at the concentration of 100 nM. With pre-treatment with MS-275 of LPS stimulated HK-2 cells, the apoptosis began to decline within a certain range. MS-275 suppressed apoptosis of LPS-stimulated HK-2 cells severely at the concentrate of 10 nM.

cytokines [27]. In the present study, we found the histological damage and dysfunction of the kidney accompanied the rise in inflammatory cytokines (TNF-α, IL-1β, IL-6, and COX-2) and ROS generation in LPS mice. ROS may induce signal transduction and then evoke apoptosis, necrosis, autophagy of several renal cells, and further exacerbate damage to the kidney. Abnormal apoptosis of renal tubular epithelial cells may affect the occurrence and progression of AKI. When cells are stimulated by harmful stimulus, large numbers of ROS are produced and the balance between oxidation and anti-oxidation system

is destroyed, and eventually oxidative stress occurs, promoting cell apoptosis and even pathological damage. Studies have shown that many kidney disease models are at the status of oxidative stress. Extracellular stimulus induces mitochondrial dysfunction and affects the activity of enzymes in the mitochondrial respiratory chain, which ultimately produces many oxygen radical. The production of active oxygen can also activate many pathways producing ROS, and active oxygen induces lipid oxidation, DNA damage, and protein degeneration [28,29].
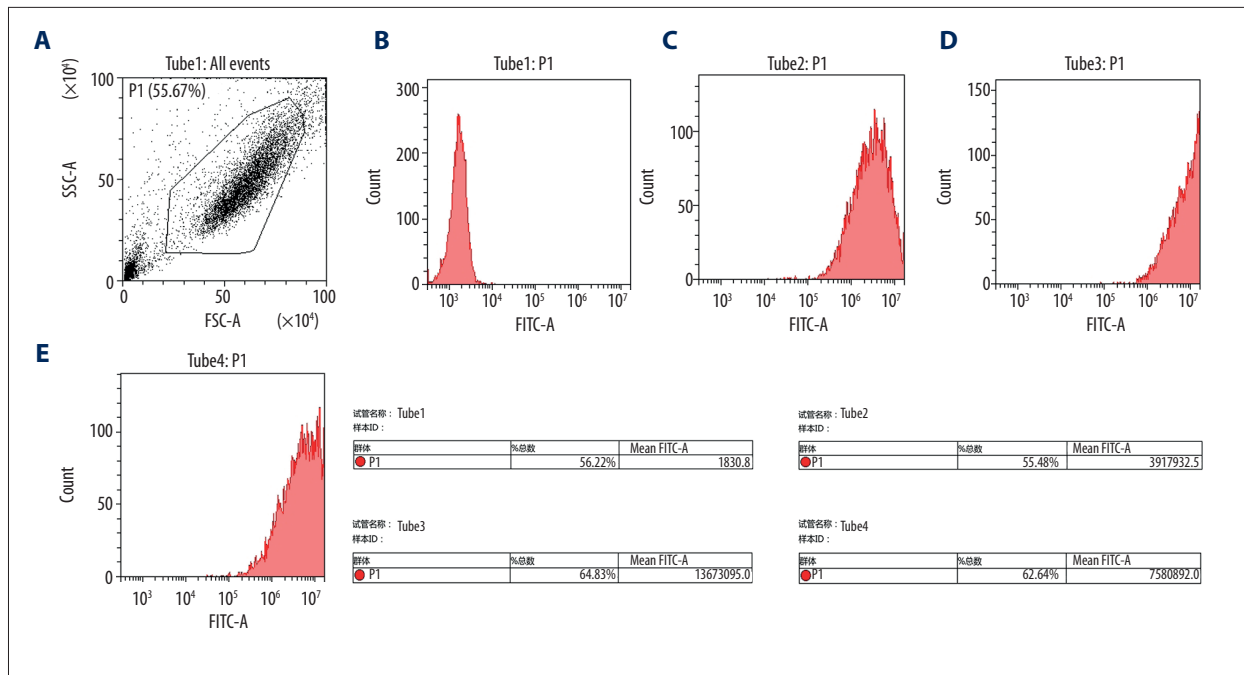
Figure 5. The generation of ROS in LPS-stimulated HK-2 cells. The production of ROS was detected by ROS assay kit and was present as mean FITC-A value in P1 region. (**A, B**) Negative control. (**C**) Normal control. (**D**) ROS expression in LPS-stimulated HK-2 cells. ROS was enhanced in the LPS group (mean FITC-A: 13673095.0) compared to the normal control group (mean FITC-A: 3917932.5). (**E**) Pre-treatment with MS-275 at the concentration of 10 nM. MS-275 suppressed the expression of ROS in LPS-stimulated HK-2 cells (mean FITC-A: 7580892.0).
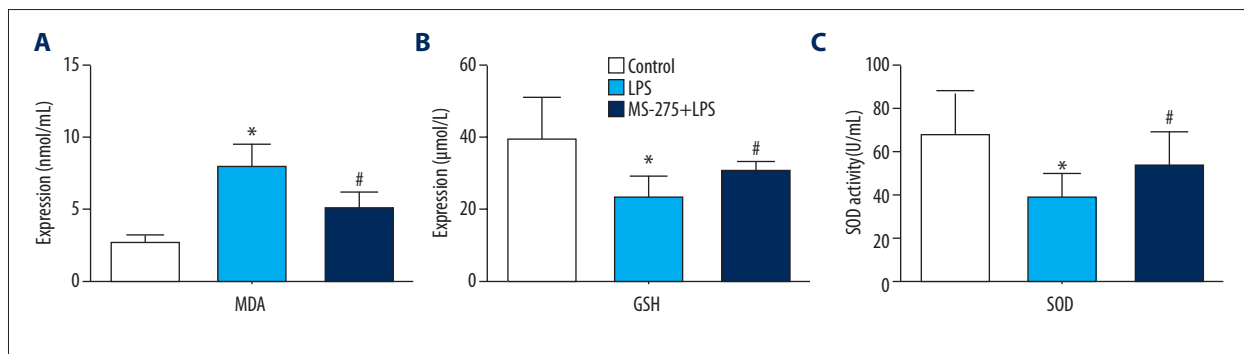

Figure 6. Oxidative stress in LPS-stimulated HK-2 cells. (**A**) The production of MDA in HK-2 cells. MDA was enhanced in LPS stimulated HK-2 cells, but suppressed by MS-275. (**B**) The production of GSH in HK-2 cells. GSH was decreased LPS stimulated HK-2 cells, but was enhanced by MS-275. (**C**) The SOD activity in HK-2 cells. SOD was decreased in LPS stimulated HK-2 cells, but was enhanced by MS-275; * $p<0.05$ versus the control group; # $p<0.05$ versus the LPS group.

ROS as an intracellular messenger activates many signaling pathways, such as the apoptosis pathway, and induces cell damage indirectly, resulting in more ROS being produced. As a result, oxidative stress is an important pathophysiological mechanism of kidney injury and participates in the development of kidney disease. Oxidative stress to the ER usually results in an accumulation of unfolded or mis-folded proteins, activating a coordinated adaptive program called unfolded protein response (UPR). The UPR is part of the process of cadmium-induced apoptosis in renal cells. Cross-talk was present between damaged ER and mitochondria; the damaged ER causes overall cellular stress which puts all organelles under threat, including mitochondria. Additionally, the activation of ER resident trans-membrane proteins by stimulating endogenous and exogenous harmful substances can activate transcription factor 6, PKR-like ER stress kinase, inositol-requiring enzyme 1, and regulate the ER stress signaling pathway [30,31]; activation of NF-κBp65 is also regulated by these pathways. Therefore, amelioration of ER stress may inhibit the inflammatory response and even improve the prognosis of septic AKI. In our study,
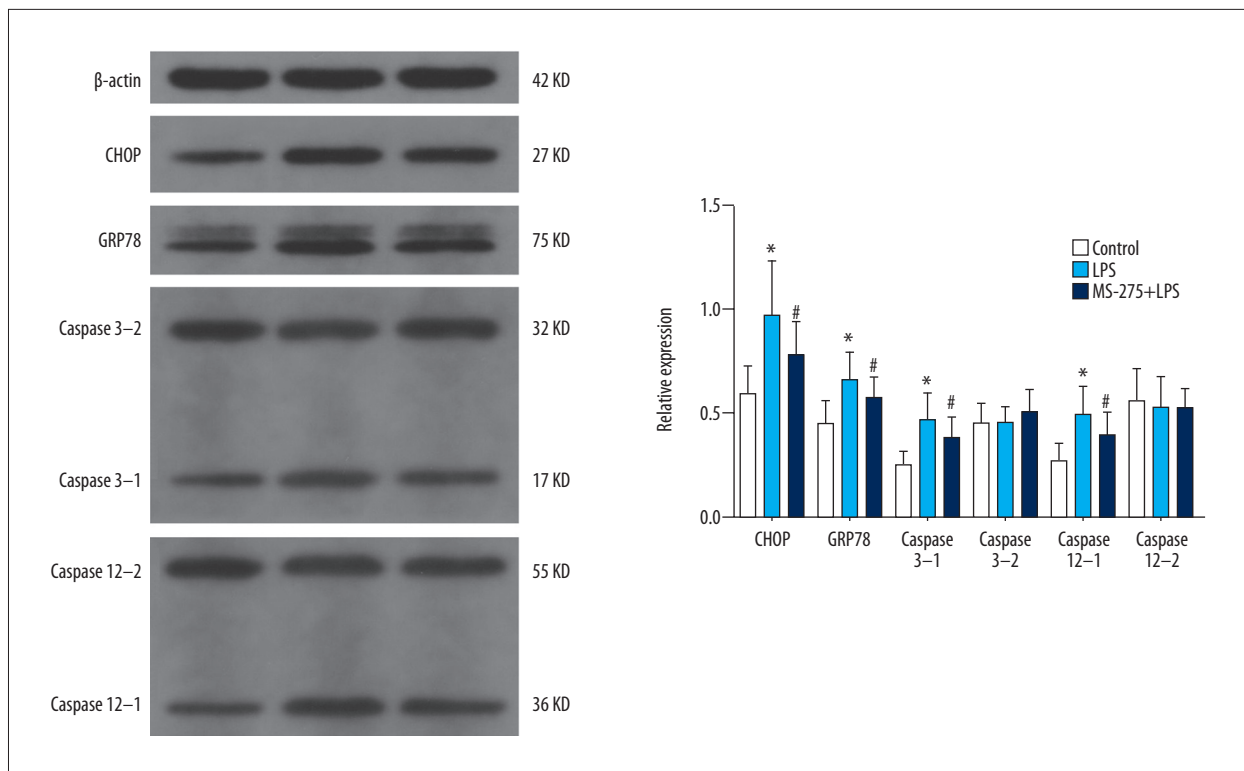
Figure 7. Endoplasmic reticulum stress and apoptosis in LPS-stimulated HK-2 cells. The expression of CHOP, GRP78, caspase3 (17KD), and caspase12 (36 KD) were enhanced in LPS-stimulated HK-2 cells, but were suppressed by MS-275; * $p < 0.05$ versus the control group; # $p < 0.05$ versus the LPS group.

the expression of NF-κBp65 in the nucleus was enhanced in LPS mice, which implied activity of NF-κBp65 in the kidney of LPS mice. NF-κB plays a key role in regulation of inflammatory cytokines transcription stimulated by LPS. Exposure to LPS leads to the activation of IKKs, phosphorylation and degradation of IκBα, and nuclear translocation and transcriptional activation of NF-κB, then activates the downstream inflammatory response pathways.

Many studies have demonstrated the significance of HDACs in LPS-inducible gene expression [32–35]. The assumed mechanism is that HDAC inhibitors may affect these processes: nucleosomal remodeling, transcription factor binding, and formation of the transcription initiation complex or transcription itself. Generally, histone acetylation is a dynamic process, which is regulated by histone acetyl transferases (HATs) and HDACs. Not only histone proteins, but transcription factors such as p53, GATA, Smad7, and NF-κB, are also subject to acetylation [36]. Nevertheless, the effect of acetylation in non-histones is not definite at this present time. It has been reported that HDACs play multiple roles during both kidney development and the pathogenesis of kidney disease. In our study, the HDAC inhibitor MS-275 attenuated the injury of renal tissue, and suppressed the generation of inflammatory cytokines and ROS in LPS mice, which implied a nephroprotective effect of MS-275 on LPS-induced AKI.

To further investigate the mechanism of nephroprotective effect of MS-275 on sepsis-induced AKI, we pretreated with MS-275 at different concentrations (0.1 nM, 1 nM, 10 nM, 100 nM) two hours before LPS-stimulus and detected the ROS generation and the related apoptosis in HK-2 cells. In the preliminary experiment, we found a low dose of MS-275 suppressed LPS-induced apoptosis in HK-2 cells; and within certain concentration ranges of MS-275, the apoptosis inhibition presented a dose-dependence. We selected the most suitable concentration of MS-275 of 10 nM for further study. In MS-275 pre-treated HK-2 cells, the generation of ROS was suppressed, the markers of oxidative stress (MDA) were also suppressed, and the antioxidants (SOD activity, GSH) were enhanced. Caspase3, the key factor in the apoptosis pathway, was suppressed by MS-275 compared to LPS-stimulated HK-2 cells. This demonstrates the effects of MS-275 in suppression of oxidative stress in LPS-stimulated HK-2 cells.

Beside oxidative stress, ER stress can also be triggered by ROS via GRP78/BiP mediated phosphorylation of IRE1 and activated CHOP, JNK, ATF4, and caspase12 to subsequently promote apoptotic cell death. GRP78, CHOP, and caspase12 are important elements in the pathway of ER-mediated apoptosis. To further verify the apoptotic pathway of HK-2 cells, we detected the protein expression of caspase12, GRP78, and CHOP in

HK-2 cells. It showed that MS-275 attenuated the LPS-induced apoptosis via ER stress-dependent pathway other than the mitochondria.

Besides apoptosis, autophagy also occurring in LPS-induced sepsis. Autophagy is an intracellular degradation system for keeping cellular homeostasis. The increased ROS also enhance autophagy by activating Beclin-1/Atg5-Atg12/LC3-II pathway in LPS-induced AKI mice. Autophagy can suppress sepsis-induced kidney injury through regulation of infection and through targeting inflammasome and type I interferon (IFN) responses [37–39]. Thus, autophagy suppresses key innate immune responses and activates a type I IFN response and promotes IL1β secretion, simultaneously. Both pro- and anti-inflammatory roles of autophagy might prevent or promote cell death through the formation of autophagosome in the kidney injury due to systemic inflammation. It is reported that there is cross-talk between autophagy and apoptosis via blc-2 family

[40,41], while, the effects of MS-275 on autophagy in sepsis need further study.

Conclusions

In conclusion, the selective class I HDAC inhibitor MS-275 suppressed the release of inflammatory medium, ameliorated the renal damage, enhanced the survival rate of LPS-induced sepsis model, and played the role of nephroprotective in sepsis-induced acute kidney injury. In our *in vitro* study, MS-275 suppressed the apoptosis of LPS-stimulated HK-2 cells, which may act through inhibiting the ROS-oxidative stress and endoplasmic reticulum stress.

Conflict of interest

None.

References:

1. Fry DE: Sepsis, systemic inflammatory response, and multiple organ dysfunction: the mystery continues. Am Surg, 2012; 78(1): 1–8

2. Weber GF, Swirski FK: Immunopathogenesis of abdominal sepsis. Langenbecks Arch Surg, 2014; 399(1): 1–9

3. Takemura R, Werb Z: Secretory products of macrophages and their physiological functions. Am J Physiol, 1984; 246(1 Pt 1): C1–9

4. Dombrovskiy VY, Martin AA, Sunderram J et al: Rapid increase in hospitalization and mortality rates for severe sepsis in the United States: A trend analysis from 1993 to 2003. Crit Care Med, 2007; 35(5): 1244–50

5. Rivers EP, Coba V, Whitmill M: Early goal-directed therapy in severe sepsis and septic shock: A contemporary review of the literature. Curr Opin Anaesthesiol, 2008; 21(2): 128–40

6. Uchino S, Kellum JA, Bellomo R et al: Beginning and ending supportive therapy for the kidney (BEST kidney) investigators. Acute renal failure in critically ill patients: A multinational, multicenter study. JAMA, 2005; 294(7): 813–18

7. Chung SD, Lai TY, Chien CT et al: Activating Nrf-2 signaling depresses unilateral ureteral obstruction-evoked mitochondrial stress-related autophagy, apoptosis and pyroptosis in kidney. PLoS One, 2012; 7(10): e47299

8. Chien CT, Lee PH, Chen CF et al: *De novo* demonstration and co-localization of free-radical production and apoptosis formation in rat kidney subjected to ischemia/reperfusion. J Am Soc Nephrol, 2001; 12(5): 973–82

9. Havasi A, Borkan SC: Apoptosis and acute kidney injury. Kidney Int, 2011; 80: 29–40

10. Devarajan P: Update on mechanisms of ischemic acute kidney injury. J Am Soc Nephrol, 2006;17: 1503–20

11. Howell GM, Gomez H, Collage RD et al: Augmenting autophagy to treat acute kidney injury during endotoxemia in mice. PLoS One, 2013; 8(7): e69520

12. Jiang M, Wei Q, Dong G et al: Autophagy in proximal tubules protects against acute kidney injury. Kidney Int, 2012; 82(12): 1271–83

13. Oberholzer C, Oberholzer A, Clare-Salzler M et al: Apoptosis in sepsis: A new target for therapeutic exploration. FASEB J, 2001; 15(6): 879–92

14. Zhuang A, Forbes JM: Stress in the kidney is the road to pERdition: Is endoplasmic reticulum stress a pathogenic mediator of diabetic nephropathy? J Endocrinol, 2014; 222(3): R97–111

15. Inagi R, Ishimoto Y, Nangaku M: Proteostasis in endoplasmic reticulum – new mechanisms in kidney disease. Nat Rev Nephrol, 2014; 10(7): 369–78

16. Zhang L, Wan J, Jiang R et al: Protective effects of trichostatin A on liver injury in septic mice. Hepatol Res, 2009; 39(9): 931–38

17. Cao W, Bao C, Padalko E et al: Acetylation of mitogen-activated protein kinase phosphatase-1 inhibits Toll-like receptor signaling. J Exp Med, 2008; 205(6): 1491–503

18. Huang L: Targeting histone deacetylases for the treatment of cancer and inflammatory diseases. J Cell Physiol, 2006; 209: 611–16

19. Mishra N, Reilly CM, Brown DR et al: Histone deacetylase inhibitors modulate renal disease in the MRL-lpr/lpr mouse. J Clin Invest, 2003; 111: 539–52

20. Chen S, Bellew C, Yao X et al: Histone deacetylase (HDAC) activity is critical for embryonic kidney gene expression, growth, and differentiation. J Biol Chem, 2011; 286: 32775–89

21. Bush EW, McKinsey TA: Protein acetylation in the cardiorenal axis: The promise of histone deacetylase inhibitors. Circ Res, 2010; 106: 272–84

22. Brilli LL, Swanhart LM, de Caestecker MP et al: HDAC inhibitors in kidney development and disease. Pediatr Nephrol, 2013; 28(10): 1909–21

23. Zhang Q, Yang F, Li X et al: Trichostatin A protects against intestinal injury in rats with acute liver failure. J Surg Res, 2016; 205(1): 1–10

24. Liu N, Zhuang S: Treatment of chronic kidney diseases with histone deacetylase inhibitors. Front Physiol, 2015; 6: 121

25. Dirkes S: Sepsis and inflammation: impact on acute kidney injury. Nephrol Nurs J, 2013; 40: 125–33

26. Cunningham PN, Dyanov HM, Park P et al: Acute renal failure in endotoxemia is caused by TNF acting directly on TNF receptor-1 in kidney. J Immunol, 2002; 168(11): 5817–23

27. Himmelfarb J, McMonagle E, Freedman S et al: Oxidative stress is increased in critically ill patients with acute renal failure. J Am Soc Nephrol, 2004; 15(9): 2449–56

28. Khoshjou F, Dadras F: Mitochondrion and its role in diabetic nephropathy. Iran J Kidney Dis, 2014; 8(5): 355–58

29. Zhang H, Zhang HM, Wu LP et al: Impaired mitochondrial complex III and melatonin responsive reactive oxygen species generation in kidney mitochondria of db/db mice. J Pineal Res, 2011; 51(3): 338–44

30. Aung HT, Schroder K, Himes SR et al: LPS regulates proinflammatory gene expression in macrophages by altering histone deacetylase expression. FASEB J, 2006; 20: 1315–27

31. Brogdon J, Xu Y, Szabo S et al: Histone deacetylase activities are required for innate immune cell control of Th1 but not Th2 effector cell function. Blood, 2007; 109: 1123–30

32. Leoni F, Zaliani A, Bertolini G et al: The antitumor histone deacetylase inhibitor suberoylanilide hydroxamic acid exhibits antiinflammatory properties via suppression of cytokines. Proc Natl Acad Sci USA, 2002; 99: 2995–3000

33. Iwata K, Tomita K, Sano H et al: Trichostatin A, a histone deacetylase inhibitor, down-regulates interleukin-12 transcription in SV-40-transformed lung epithelial cells. Cell Immunol, 2002; 218: 26–33

34. Ma T, Han L, Gao Y et al: The endoplasmic reticulum stress-mediated apoptosis signal pathway is involved in sepsis-induced abnormal lymphocyte apoptosis. Eur Surg Res, 2008; 41: 219–25

35. Esposito V, Grosjean F, Tan J et al: CHOP deficiency results in elevated lipopolysaccharide-induced inflammation and kidney injury. Am J Physiol Renal Physiol, 2013; 304: F440–50

36. Chen LF, Greene WC: Regulation of distinct biological activities of the NF-kappaB transcription factor complex by acetylation. J Mol Med, 2003; 81: 549–57

37. Deretic V, Kimura T, Timmins G et al: Immunologic manifestations of autophagy. J Clin Invest, 2015; 125(1): 75–84

38. Lee HK, Lund JM, Ramanathan B et al: Autophagy-dependent viral recognition by plasmacytoid dendritic cells. Science, 2007; 315(5817): 1398–401

39. Kimura T, Jain A, Choi SW et al: TRIM-mediated precision autophagy targets cytoplasmic regulators of innate immunity. J Cell Biol, 2015; 210(6): 973–89

40. Fink SL, Cookson BT: Pyroptosis and host cell death responses during Salmonella infection. Cell Microbiol, 2007; 9(11): 2562–70

41. Orrenius S, Nicotera P, Zhivotovsky B: Cell death mechanisms and their implications in toxicology. Toxicol Sci, 2011; 119(1): 3–19